

**2018 NDIA GROUND VEHICLE SYSTEMS ENGINEERING AND TECHNOLOGY
SYMPOSIUM
MATERIALS & ADVANCE MANUFACTURING (M&AM) TECHNICAL SESSION
AUGUST 7-9, 2018 - NOVI, MICHIGAN**

**DISSIMILAR FRICTION STIR WELDING OF A SOLID SOLUTION-
STRAIN HARDENED ALUMINUM 5083 ALLOY AND PRECIPITATION
STRENGTHENED ALUMINUM 2139 AND ALUMINUM 7085**

Nelson Martinez, PhD
Concurrent Technologies Corporation
Johnstown, PA

Martin McDonnell
US Army TARDEC
Warren, MI

ABSTRACT

Friction stir welding is a solid state joining technique in which no melting of the metals is involved. The technique is very attractive for aluminum alloys due to the low heat input involved in the process, which leads to improved mechanical properties as compared to conventional fusion welds. In this work, different aluminum series alloys were friction stir welded together. The aluminum alloys consisted of a solid solution/strain hardened aluminum alloy 5083-H131, and precipitation strengthened aluminum alloys 2139-T8 and aluminum 7085-T721. The joint combinations were aluminum alloys 5083-H131 to 7085-T721, aluminum alloys 2139-T8 to 7085-T721, and aluminum alloys 5083-H131 to 2139-T8. Their mechanical properties were analyzed and compared to base metal properties. Optical microscopy was used to analyze the grains in the welds. Good mixing of the different aluminum alloys was optically observed in all of the welds, which lead to good joint properties, opening the possibilities to build structures with superior performance.

INTRODUCTION

Friction stir welding (FSW) is a solid state joining technique in which no melting of the materials is involved, eliminating the complications associated with the liquid-to-solid state phase transition, such as solidification shrinkage pores, solidification/liquation cracking, and unwanted intermetallic formation [1]. Furthermore, compared to conventional fusion methods, FSW consumes less energy, there is no need for filler materials, and no shielding gas is required [1-2].

Aluminum alloys (AA) are an attractive option for manufacturing of military systems, due to their optimized weight efficiency ratio [3]. The most common alloy used for current systems is AA5083-

H131, which is a solid solution strengthened aluminum alloy [4]. It is typically strain hardened for optimum strength, hence the H131 designation. It is light weight, has good corrosion resistance, and is considered a weldable alloy. As ground vehicle system level requirements (i.e. increased survivability and light weighting) continue to change, more advanced high strength aluminum grades such as AA2xxx and AA7xxx series alloys are needed.

Recently designed aluminum armored based vehicles, have incorporated higher strength aluminum alloys for increased ballistic protection. One such alloy is AA2139-T8, which is a precipitation strengthened alloy [5]. Its main

strengthening precipitate is the Ω (Al_2Cu) phase. The Ω precipitate nucleates homogeneously in the grain matrix, which leads to less grain boundary precipitation and reduces the chances of intergranular fracture. AA7085-T721 is also precipitation strengthened and its main strengthening precipitate is the η' (MgZn_2) phase [6-7]. These alloys are considered unweldable with conventional fusion techniques due to the excess detrimental effects associated with the liquid to solid phase transition. Therefore, friction stir welding has emerged as the preferred technique for joining aluminum alloys due to it being a solid state/low heat input process.

FSW of dissimilar aluminum alloys provides a method of manufacturing to meet strength and performance requirements in specific areas that would otherwise not be achieved through arc welding. During FSW, three distinct microstructural zones develop: the stir zone (nugget), thermo-mechanical affected zone (TMAZ), and the heat affected zone (HAZ) [1, 7]. The stir zone experiences extensive plastic deformation and high heat input, resulting in a recrystallized microstructure. The TMAZ serves as the transition between the nugget and heat affected zone. The HAZ is the zone that experiences elevated temperatures but no plastic deformation. The effect of the temperature rise in this zone typically leads to reduction in strength, making it the weakest region of the weld. In AAxxx and AA7xxx, the strengthening precipitates either dissolve or coarsen, while the AA5xxx suffers from softening when heat is applied.

In this work, dissimilar friction stir welds of different aluminum alloys were carried out. The thermal and mechanical effects on AA5083-H131, AA2139-T8, and AA7085-T721 have been analyzed. Particular attention was placed in the nugget and HAZ. The nugget was of particular interest, since this is where the mixing of the different aluminum alloys occurred. Effective joining in this region is crucial. The HAZ was also

of prime interest since this is where the weakest region of the weld is typically observed. Adequate strength in these regions is needed to obtain good performance for structural applications such as military systems [8].

MATERIALS AND METHODS

The alloys used in this work consisted of a solid solution/strain hardened AA5083-H131 alloy, and precipitation strengthened AA 2139-T8 and AA7085-T721 (Figure 1). The FSW tool consisted of a MP159 Ni-Co based alloy. The tool was tapered down and had 5 flats to promote mixing. The plates were friction stir welded together in a butt joint configuration and consisted of plates that were 2" thick, 24" long, and 6" wide. Figure 2 shows the FSW process during welding.



Figure 1: Tool MP159 with 5 flats.

Their mechanical properties were analyzed through tensile, side bend, and micro hardness testing. Both macro and optical microscopy were used to analyze the welds for mixing and grain size. The samples were final polished with .05 micron silica. Etching was done according to the alloy: AA7085-T721 was etched with Keller's reagent, AA2139-T8 was etched with diluted Keller's with glycerol, and AA5083-H131 was etched with electrolytic Barkers etch.



Figure 2: Friction stir welding process.

RESULTS

Three different welds were made and characterized. The different combinations included AA2139-T8 to AA7085-T721, AA5083-H131 to AA7085-T721, and AA5083-H131 to AA2139-T8.

Aluminum 2139-T8 to Aluminum 7085-T721

The first set of welds consisted of AA7085-T721 to AA2139-T8. The AA7085-T721 was placed on the retreating side of the tool and the AA2139-T8 was placed in the advancing side of the tool. The rotational spindle speed was 110 RPM (revolutions/minute) and tool velocity of 2 IPM (inches/minute).

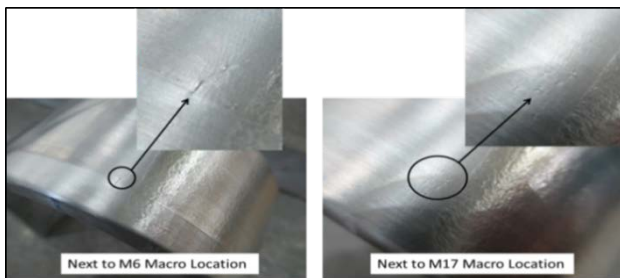


Figure 3: AA2139-T8 to AA7085-T721 bend test result.

The machined macro specimens did not show any visual defects in the weld. Bend specimens located next to the macro cross-sections were fabricated and tested. Figure 3 shows the bend specimen results. As observed in the images, there were some minor cracks noted at the weld nugget advancing side interface in the bend specimens. However, the Dissimilar Friction Stir Welding of a Solid Solution-Strain Hardened Aluminum 5083 Alloy and Precipitation Strengthened Aluminum 2139 and Aluminum 7085, Martinez, et al.

bend tests were considered a pass, since the cracks were very minor.

Three tensile specimens were fabricated from the middle section of the welded plate and tested. The average tensile strength and average elongation of the specimens were 46.9 ksi and 12.7 ksi respectively. Table 1 shows the tensile results for the welds as compared to the base metals. Figure 4 shows the three broken tensile specimens. All three tensile specimens broke on the retreating side of the weld, in the AA7085-T721 HAZ.



Figure 4: A2139-T8 to AA7085-T721 tensile test result.

Table 1: Tensile test summary for AA2139-T8 and AA7085-T721.

Sample	Ultimate Stress (ksi)	Yield Stress (ksi)	% EL
7085-T721	68	60	12
2139-T8	67	64	9
2139-T8 to 7085-T721	46.9	31.1	12.7

Figure 5 shows the macro image of the AA2139-T8 to AA7085-T721. As observed from the image, there are no pores or cracks, indicating that there was good mixing of the two metals. Since there was no failure in the nugget, it does appear there is a locking mechanism in place joining the two different alloys. However, there does appear to be a clear division between the AA2139-T8 and AA7085-T721 within the nugget as observed.

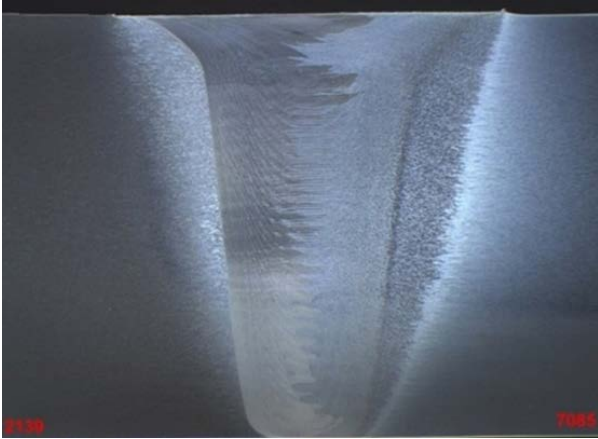


Figure 5: Macro image of 2 in. AA2139-T8 and AA7085-T721.

Figure 6 shows the hardness profiles for the top, middle, and bottom of the weld. As observed from the hardness profiles, the weakest part of the weld was in the HAZ of the AA7085 (~88 HV). Furthermore, there is a clear division in hardness values observed in the nugget (the values average 130 HV in the AA2139-T8 nugget while the AA7085-T721 average 160 HV). Clearly there is a division between the two aluminum alloys in the nugget.

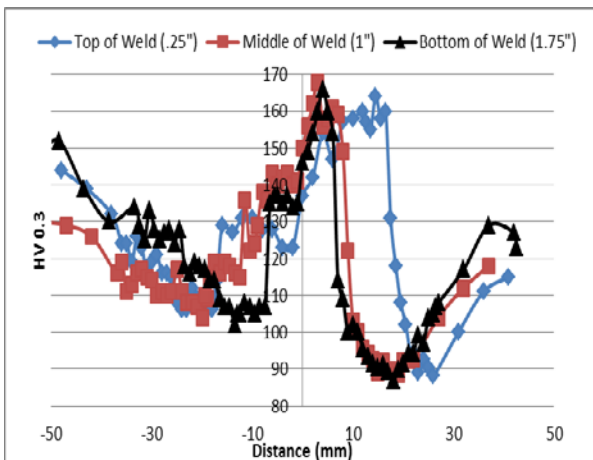


Figure 6: Hardness profile for AA2139-T8 to AA7085-T721.

The effects of the heat on the base metal are clearly visible, as can be observed by the shaded coloring (outside of the nugget of Figure 5) in the HAZ region for both alloys. As was observed by the tensile tests, failure occurred in the HAZ of the

Dissimilar Friction Stir Welding of a Solid Solution-Strain Hardened Aluminum 5083 Alloy and Precipitation Strengthened Aluminum 2139 and Aluminum 7085, Martinez, et al.

AA7085-T721. This indicates that the dissipation of heat is more detrimental on the AA7085-T721 alloy.

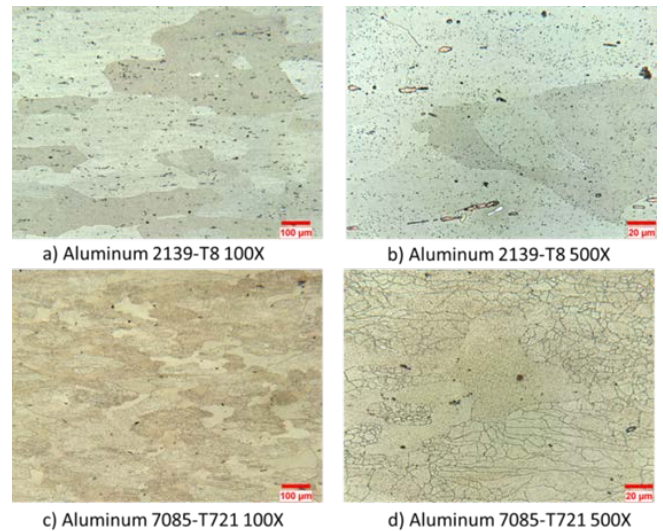


Figure 7: AA2139-T8 at a) 100X and b) 500 X, and AA7085-T721 at c) 100X and d) 500X.

Figure 8 shows the optical images of the nugget. Hardness values were taken along the depth of the nugget from three different depths: the top of weld (.25 inch from the top), middle of weld (1 inch from the top), and bottom of weld (1.75 inch from top). The X-axis is the distance between each hardness indentation. From the images, there appears to be recrystallization of the existing parent material grains (Figure 7) into finer grains. However, the optical images do show a clear separation of the grains between the AA2139-T8 and AA7085-T721.

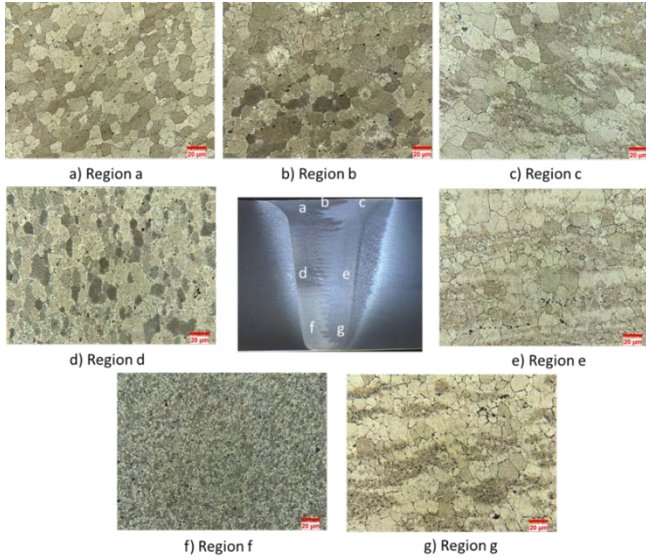


Figure 8: Nugget of 2 in. AA2139-T8 to AA7085-T721 at 500X region a,b,d,f) consists of finer grains pertaining to AA 139-T8 and region c,e,g) consist of fine finer grains pertaining to AA7085-T721.

Aluminum 5083-H131 to Aluminum 7085-T721

The second set of joints consisted of AA5083-H131 to AA7085-T721. A starting spindle speed of 120 RPM was selected as the starting point, and a final decreasing spindle speed of 110 RPM, since it was expected that it would provide less heat with reduction in rotational rate. The tool velocity was kept at 1.8 IPM.

Macros were taken from weld positions at the 120 RPM and 110 RPM sections. The machined macros sections did not show any defects in the weld nugget or areas adjacent to it as shown in Figure 8. Material for bend specimens was taken from the weld plate just ahead of where each macro cross-sections sample was taken. In the bend specimen taken from the 120 RPM section, there were minor cracks on the advancing side of the AA5083-H131 alloy near the top. There were also minor cracks on the retreating side of the AA7085-T721, at the top in the heat affected zone. The bend specimen from the 110 RPM section showed the same results as the 120 RPM specimen, but the cracks were not as visible and open. None of the weld nugget cracks extended through the bend specimen thickness.

Dissimilar Friction Stir Welding of a Solid Solution-Strain Hardened Aluminum 5083 Alloy and Precipitation Strengthened Aluminum 2139 and Aluminum 7085, Martinez, et al.

Figure 9 shows the tested bend specimens from the 120 and 110 RPM, respectively. Since the cracks were minor, the bend tests were considered a pass.



Figure 9: AA5083-H131 to AA7085-T721 bends test results at a) 120 and b) 110 rpm.

One tensile specimen was fabricated from each of the RPM sections (120 and 110) of the welded plate and tested. The tensile results are show in Table 2. The tensile specimens from the 120 RPM and 110 RPM sections broke outside the weld nugget on the retreating side of the AA7085-T721 in the heat affected zone. Again, the HAZ of the AA7085-T721 is the weakest region of the weld, and where failure occurs.

Table 2: Tensile test summary for AA5083-H131 and AA7085-T721.

Sample	Ultimate Stress (ksi)	Yield Stress (ksi)	% EL
AA7085	68	60	12
AA5083	45	37	8
AA5083-7085 (120 RPM)	46.2	25.7	16.1
AA5083-7085 (110 RPM)	46.4	26.2	19.1

Figure 10 shows the macro image of AA5083-H131 to AA7085-T721. As observed from the image, there are no pores or cracks, indicating that there was efficient mixing of the two metals. Furthermore, there does appear to be a clear division from the AA5083-H131 and the AA7085-T721 as was observed with the first weld (AA2139-T8 to AA7085-T721).

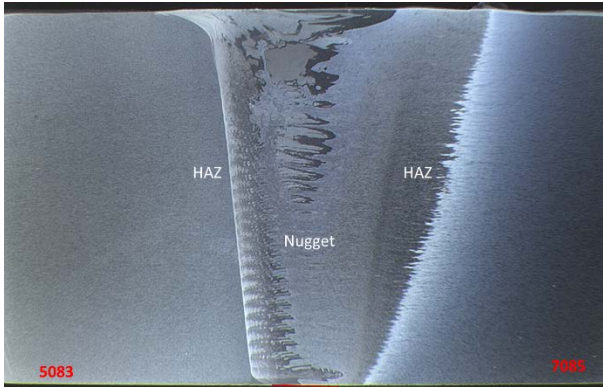


Figure 10: Macro image of 2 in. AA5083-H131 and AA7085-T721.

An interlocking mechanism appears to be the reason for the joining of the two different alloys, similar to the AA2139-T8 to AA7085-T721 welds. The effects of heat on the base metal are visible on the AA7085-T721 alloy, as can be observed by the shaded region of the HAZ. However, such is not the case for the AA5083-H131 alloy. This indicates that the negative effects due to the dissipation of heat in the HAZ of the AA5083-H131 were minor. This is confirmed by the tensile test for these dissimilar welds; all failed in the HAZ of the AA7085-T721.

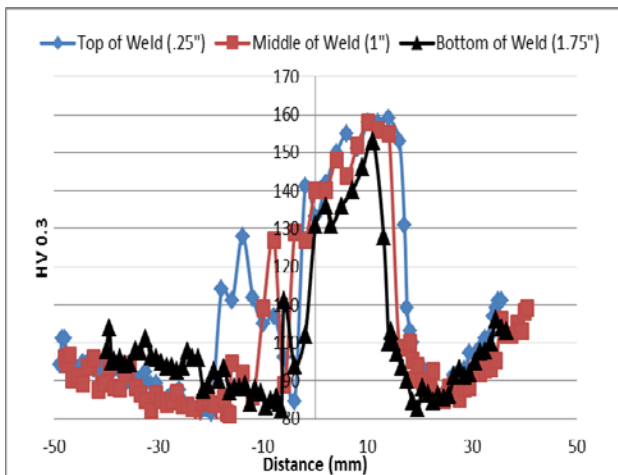
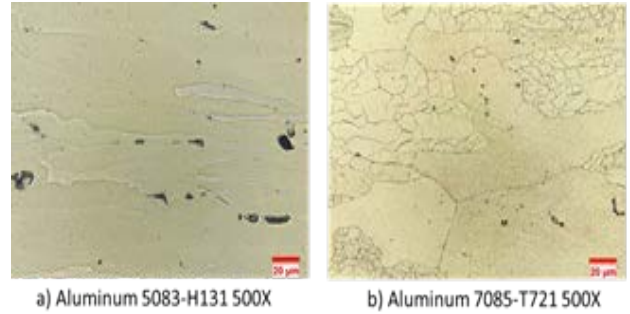


Figure 11: Hardness profile for AA5083-H131 to AA7085-T721.

Figure 11 shows the hardness profiles at the top, middle and bottom of the weld. Similar to the previous weld, a division in hardness values is observed in the nugget.

Dissimilar Friction Stir Welding of a Solid Solution-Strain Hardened Aluminum 5083 Alloy and Precipitation Strengthened Aluminum 2139 and Aluminum 7085, Martinez, et al.



a) Aluminum 5083-H131 500X

b) Aluminum 7085-T721 500X

Figure 12: a) AA5083-H131 at 500X, and b) AA7085-T721 at 500X.

The optical images (Figure 13) also show the grains in the nugget appear to consist of a mixture of the two different alloys.

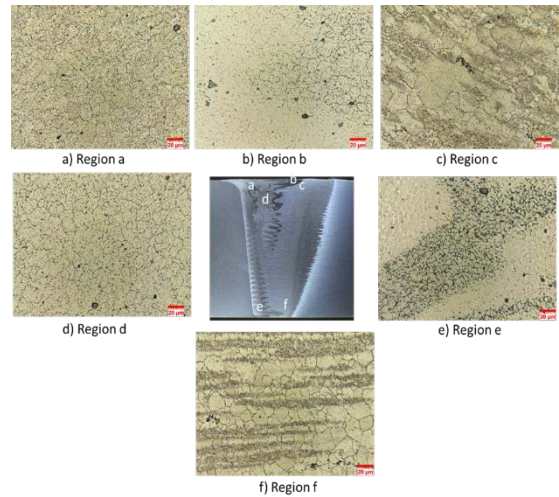


Figure 13: Nugget 5083-H131 to 7085-T721 at 500X region a,b,d,e) consists of finer grains pertaining to AA 5083-H131 and region c,f) consist of fine finer grains pertaining to AA 7085-T721.

Furthermore, there is recrystallization observed for both metals. As can be observed, the grains in the nugget are finer as compared to the base metal grains (Figure 12), which is similar to what was observed for the first set of dissimilar welds (AA2139-T8 to AA7085-T721).

Aluminum 5083-H131 to Aluminum 2139-T8

The third set of joints consisted of AA5083-H131 to AA2139-T8. A spindle speed of 110 RPM was selected. The tool velocity was kept at 1.8 IPM.

Table 3: Tensile test summary for Al 5083-H131 and 2139-T8.

Sample	Ultimate Stress (ksi)	Yield Stress (ksi)	Elong (%)
5083	45	37	8
2139	67	64	9
2139-5083	48.6	28	11.8

Tensile specimens were fabricated from a section of the welded plate and tested. The average tensile strength of the specimens was 48.6 ksi. Table 3 shows the tensile results for the welds as compared to the base metals. All tensile specimens broke on the HAZ of the AA5083-H131 side of the weld. This indicates that the weakest section of the weld was outside the AA5083-H131 in the HAZ. Even though AA5083-H131 does not contain strengthening precipitates, there is a reduction in strength due to the heat effects.



Figure 14: Macro image of Al 5083-H131 and Al 2139-T8.

Figure 14 shows the macro image of the AA5083-H131 to AA2139-T8. As observed from the image, there are no pores or cracks, indicating that there was good mixing of the two metals. Furthermore, it does appear there is a locking mechanism in place joining the two different alloys. However, a clear division between the AA5083-H131 and AA2139-T8 within the nugget is observed, as was the case with the first two dissimilar welds.

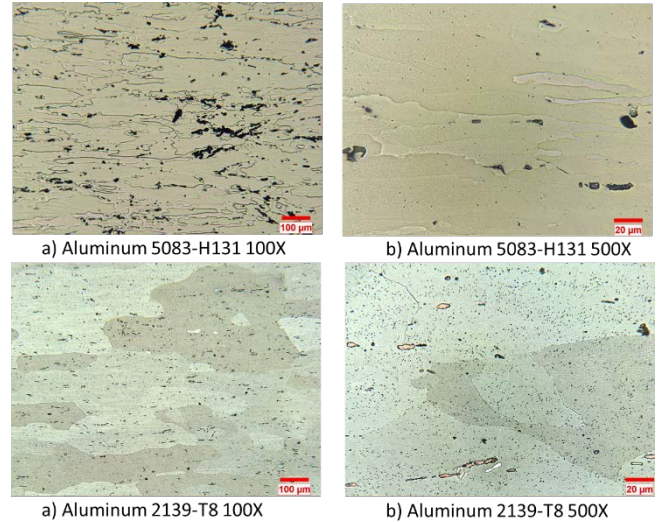


Figure 15: AA5083-H131 at a) 100X and b) 500 X, and AA2139-T8 at c) 100X and d) 500X.

Figure 16 shows the optical images of the nugget. From the images, there appears to be recrystallization of the existing parent material grains (Figure 15) into finer grains.

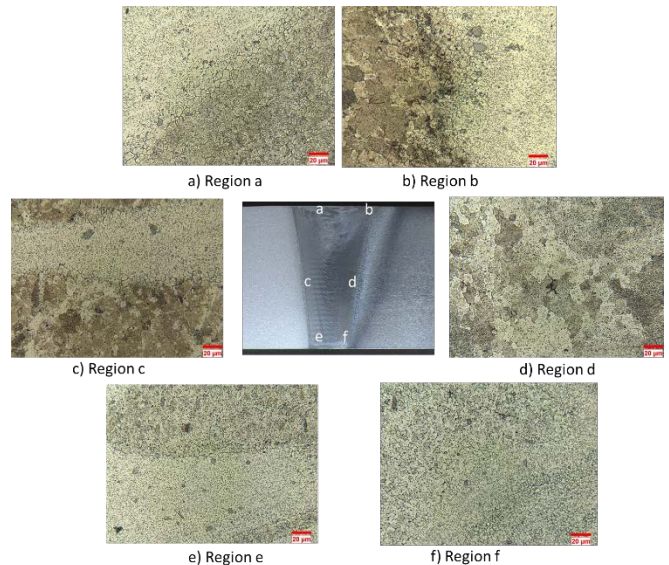


Figure 16: Nugget 5083-H131 to 2139-T8 at 500X region a,b,c,e) consists of finer grains pertaining to a mixture of AA 5083-H131 and AA 2139-T8 and region d,f) consist of fine finer grains pertaining to AA 2139-T8.

From the optical images, it can be observed that there are certain regions of the weld where there is

a clear division between the grains of the two alloys. Figure 16 shows this division.

DISCUSSION

The bend test, tensile test, and optical microscopy show there is an effective interlock joining the dissimilar aluminum alloys. Furthermore, failure does not occur in the nugget of the welds, indicating FSW is a very effective method to join dissimilar aluminum alloys, which are currently used in military vehicles.

Thermal Dissipation

The joint efficiency of friction stir welded dissimilar aluminum is ultimately dictated by the heat dissipated throughout the weld. The amount of heat and plastic deformation in the nugget will dictate the effectiveness for interlocking. Overall, the heat in the nugget will be higher than the heat in the TMAZ and HAZ. However, the HAZ is where the most detrimental effects due to the temperature rise occurs (lowest strength is observed).

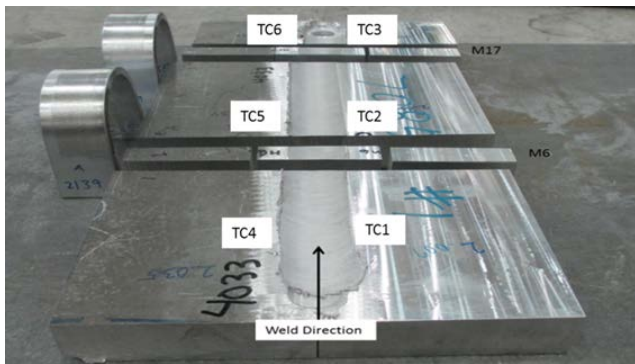


Figure 17: Position of placement of thermocouples for thermal measurements during the weld.

The loss in strength will differ for each alloy; mostly depending on the pre-existing microstructure (precipitates, dislocations, grains), as well as any change that occurs during the weld. The amount of damage in the HAZ depends on the amount of heat input, peak temp reached, distance from the nugget, time at elevated temp, cooling

Dissimilar Friction Stir Welding of a Solid Solution-Strain Hardened Aluminum 5083 Alloy and Precipitation Strengthened Aluminum 2139 and Aluminum 7085, Martinez, et al.

rate, and the base metal’s thermal properties. Hence, analysis of the heat dissipation through the metals is needed to fully understand the effects it has on the properties.

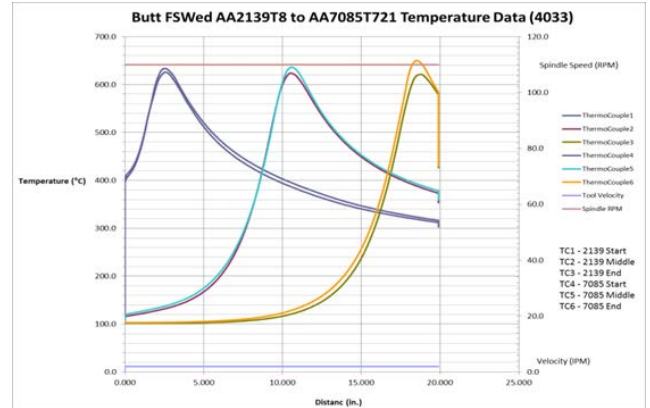


Figure 18: Thermal measurements of AA2139-T8 to AA7085-T721.

Thermal measurements were taken at the top of the welds, outside the shoulder for the AA2139-T8 to AA7085-T721 and for the AA5083-H131 to aluminum AA7085-T721. Figure 17 shows the position of the thermal couples. Figure 18 and Figure 19 show the thermal profiles for the dissimilar welds.

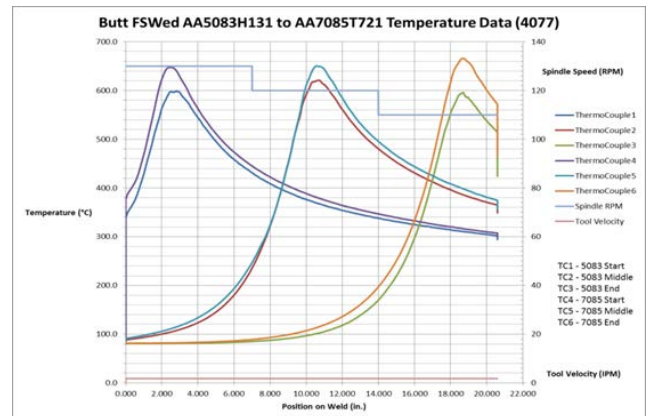


Figure 19: Thermal measurements of AA5083-H131 to AA7085-T721.

The data shows the temperature reaches approximately 650 °C outside in the HAZ near the shoulder for all dissimilar welds. The thermal profiles do show a slightly lower temperature for

the retreating side of the welds. However, as can be observed from the graphs, the temperature jumps to 650 °C, but reduces relatively quickly to approximately 350 °C. The timing of a temperature rise is relatively short in the HAZ. However, the nugget will have a higher temperature rise and longer timing compared to the HAZ.

Nugget Recrystallization/ Re-precipitation

It is clear from the optical images that a division between the two different aluminum alloys ensues in the nugget. Similar results were also observed by Ilangoan et al. in their work with AA6061 to AA5086 [9]. However, there is a form of interlocking between the alloys, and it is this interlock mechanism that joins them together (all the different combination AA2139-T8 to AA7085-T721, AA5083-H131 to AA2139-T8, and AA508-H131 to AA7085-T721 showed this).

Even though the alloys join via an interlocking mechanism in the nugget, the alloys do experience recrystallization and re-precipitation. The intense plastic deformation and high temperature reached in the nugget causes a high degree of dissolution of the existing microstructure (the majority of the existing precipitates and grains in the aluminum will be wiped out) [10-11]. During the cooling stage of the weld, recrystallization and re-precipitation occurs, leading to regains in strength. From the optical images, there does appear to be a new set of finer grains, which differ from the parent materials for all the aluminum alloys. However, each alloy recrystallizes and re-precipitates independent of the others.

The AA5083-H131 is a solid solution /strain hardened alloy. Due to the intense plastic deformation and high temperature experienced, there should be dissolution of the existing grains and the existing constituent particles. During the cooling stages of the weld there is redistribution of the solute in the nugget, and a new set of finer equiaxed grains form. This new microstructure is not as strong as the base metal, since there is a loss

in strain hardening, but it is strong enough that failure does not occur in the nugget.

AA2139-T8 and AA7085-T721 alloys are strengthened by fine metastable precipitates. AA2139-T8 is strengthened by the Ω phase, while AA7085-T721 is strengthened by the η' phase. During FSW, these precipitates dissolve and re-precipitate. Furthermore, recrystallization does occur in these alloys as well. However, since aluminum typically does not depend on grain strengthening, very little effect on the strength of the nugget is expected.

It appears that the nugget should have a mixture of the precipitates, grains, and solute due to the interlock mechanism. Overall, it appears that the nugget recovers high enough strength that failure does not occur when under tensile load. Again, this analysis indicates that FSW is very effective for joining dissimilar aluminum alloys. However, the heat affected zone does exhibit lower strength and it is where failure usually occurs for the dissimilar welds.

Heat Affected Zone-HAZ

From the tensile tests, the precipitation strengthened AA7085-T721 fails at the HAZ for both dissimilar combinations (AA5083-H131 to AA7085-T721 and AA2139-T8 to AA7085-T721). The results show that the weakest region of the weld is the HAZ of the precipitation strengthened AA7085-T721. Furthermore, it appears that the AA5083-H131 is able to withstand the heat effects better than the precipitation strengthened AA7085-T721; none of the tensile test showed failure in the HAZ of the AA5083-H131. However, the AA5083-H131 to AA2139-T8 welds showed failure in the HAZ of the AA5083-H131. It is expected for the AA5083-H131 suffers a reduction in strength due to the heat experienced in the HAZ.

When heat dissipates through the AA5083-H131, a relief in internal strain energy and reduction in dislocation density should occur. However, FSW is a relatively low heat input process and the timing

under elevated temperatures is short as was observed in the thermal profiles (Figure 18 and Figure 19). The heat effect on the HAZ does not have an extensive detrimental effect on the AA5083-H131 alloy, as it did on the AA2139-T8 and the AA7085-T721.

As mentioned earlier, the AA7085-T721 is strengthened by η' and the AA2139-T8 is strengthened by the Ω phase. In the HAZ, there is dissolution and coarsening of the existing precipitates resulting in strength reduction [12]. It does appear from the tensile tests that the precipitates (Ω) in the AA2xxx series survived the effects of the heat better than the η' in AA7085-T721. This could be due to the size of the precipitates. Larger, more stable precipitates survive the heat effects better during the weld, while finer less stable precipitates dissolve easier. From this work, the Ω phase survives the heat effects better than the η' phase, since failure did not occur in the AA2139-T8 during tensile testing.

CONCLUSION

In this study, the feasibility of FSW for joining dissimilar aluminum armor alloys was investigated. Good intermixing of the aluminum alloys was microscopically observed. Electron backscatter diffraction (EBSD) is still needed for proper grain size measurements and to validate the dissolving or coarsening of precipitates in the AA2xxx and AA7xxx alloys.

It has also been shown, that the weakest region of the 3 different combinations (AA5083-H131 to AA7085-T721, AA2139-T8 to AA7085-T721, and AA5083-H131 to AA2139-T8) is the HAZ. The dissipation of the heat through the aluminum alloys, and the effect the heat has on the HAZ ultimately dictates the strength of the weld. Future work needs to focus on methods to improve the HAZ. One possible solution may be the addition of a chilling process during FSW to better regulate the heat input and cooling rates of the alloy. Also, a post weld

heat treatment could help improve the strength in the HAZ.

Overall, this work does show that FSW is a great option to build the next generation military vehicles.

REFERENCES

- [1] R. S. Mishra and Z. Y. Ma, "Friction Stir Welding and Processing," Materials Science and Engineering: R: Reports, Elsevier, Jan 2005.
- [2] C. R. Breivik, "Mechanical Properties of Gas Metal Arc and Friction Stir AA6082-T6 Weldments", MS Thesis, Institute for Materials Technology, 2013
- [3] J.R Davis, "Aluminum and Aluminum Alloys", Alloying: Understanding the Basics, ASM International, pages 351-416, 2001.
- [4] J. Buczynski "Electrochemical Analysis of Etchants Used to Detect Sensitization in Marine-Grade 5XXX Aluminum-Magnesium Alloys" MS Thesis, University of Virginia, 2012
- [5] C. Velotti, A. Astarita, P. Buonadonna, G. Dionoro "FSW of AA 2139 plates: influence of the temper state on the mechanical properties" Key Engineering Materials, Vols. 554-557, pp 1065-1074, 2013
- [6] T. Ram Prabhu, "An Overview of High Performance Aircraft Structural Al Alloy-AA7085" Acta Metall. Sin (Eng. Lett), Springer, 28 (7), 2015
- [7] D. Gallardy "Ballistic Evaluation of 7085 Aluminum" Army Research Laboratory, ARL-TR 5952, 2012
- [8] M. Grujicic, G. Arakere, B. Pandurangan, A. Hariharan, C.-F. Yen, and B.A. Cheeseman, "Development of a Robust and Cost-Effective Friction Stir Welding Process for Use in Advanced Military Vehicles" Journal of Materials Engineering and Performance, ASM International (20) pp 11-23, 2011

- [9] M. Ilangoan, S. Rajendra Boopathy, and V. Balasubramanian, "Effect of Tool Pin Profile on Microstructure and Tensile Properties of Friction Stir Welded Dissimilar AA6061-AA5086 Aluminum Alloy Joints" *Defense Technology*, Elsevier (11) pp 174-184, 2015
- [10] J.Q. Su, T.W. Nelson, R. Mishra, M. Mahoney, "Microstructural Investigation of Friction Stir Welded 7050-T651 Aluminum", *Acta Mater.* 51 (3) pp 713-729 (2003)
- [11] N. Martinez, N. Kumar, R.S. Mishra, K.J Doherty, "Microstructural Variation Due to Heat Gradient of a Thick Friction Stir Welded Aluminum 7449 Alloy" *Journal of Alloys and Compounds*: 713 pp 51-63 (2017)
- [12] N. Martinez, N. Kumar, R.S. Mishra, K.J Doherty, "Effect of Tool Dimensions and Parameters on the Microstructure of Friction Stir Welded Aluminum 7449 Alloy of Various Thicknesses" *Material Science and Engineering: A* 684 pp 470-479 (2017)

Dissimilar Friction Stir Welding of a Solid Solution-Strain Hardened Aluminum 5083 Alloy and Precipitation Strengthened Aluminum 2139 and Aluminum 7085, Martinez, et al.